International Journal of Technology 15(1) 39-48 (2024)
Received October 2022 / Revised December 2022 / Accepted March 2023

International Journal of Technology

http://ijtech.eng.ui.ac.id

The Effect of Alumina Nanoparticles Impregnated Kevlar on Ballistic Resistance of Aluminum Alloy 7075 Hybrid Laminate Composite for Armor Application

Salsabila Syifa[1], Myrna Ariaty[1], Anne Zulfia Syahrial[1*], Agus Pramono[2]

[1]*Composites Laboratory, Department of Metallurgical and Materials Engineering, Faculty of Engineering, Universitas Indonesia, Kampus Baru UI, Depok 16424, Indonesia*
[2]*Department of Metallurgical Engineering, Faculty of Engineering, Universitas Sultan Ageng Tirtayasa Jl. Jenderal Sudirman Km 3, Kotabumi, Cilegon, Banten 42435 Indonesia*

Abstract. Military equipment development, especially means of transportation, currently revolves around material selection, which includes hybrid laminate composite as a prominent material choice due to its strength-to-weight ratio. The hybrid laminate composite was fabricated by involving aluminum alloy 7075-T6 sheets and Kevlar fabrics that were introduced to shear thickening fluid (STF). STF was made by mixing PEG-400, alumina nanoparticles, and ethanol in a certain ratio. The composites were fabricated using variations of Kevlar layers of 8, 16, and 24 layers. Ballistic impact resistance of the hybrid laminate composite was observed through a ballistic test that was performed according to the National Institute of Justice (NIJ) 1080.01 level II standard. The energy absorption of the composites was evaluated by analyzing the diameter of the perforation. Additionally, the failure mode of the Al7075 matrix and Kevlar fabric are discussed. The findings from ballistic testing indicated that the addition of alumina nanoparticles into three variations of Kevlar layers in hybrid laminate composite yielded the improvement of ballistic performance and impact energy of the composites.

Keywords: Alumina; Ballistic performance; Hybrid laminate composite; Shear thickening fluid

1. Introduction

The latest trend in the improvement of military equipment is focusing on the development of material selection for ballistic protection, especially for vehicles such as tanks. However, to produce an ideal tank, fuel consumption and vehicle agility must be taken into consideration. In order to be used as an armor material, the composite should have ballistic performance. The typical steel used for armor material can be replaced by the aluminum alloy 7075-T6, which has major applications in the military industry (Senthil *et al.*, 2017). Studies prove that AA 7075-T6 has better ballistic performance compared to AA 2024 and AA 6061(Yeter, 2018). To further enhance the energy absorption ability, Kevlar, which is well-known for its high strength and other mechanical properties that are comparable with steel, was involved. A study demonstrates that a hybrid laminate composite treated with nanoparticles increases energy absorption based on a ballistic test (Haro, Szpunar, and Odeshi, 2016a). Nanoparticles are used as the constituent of shear

*Corresponding author's email: anne.zulfia@ui.ac.id, Tel.:+217863510; Fax.: +217872350
doi: 10.14716/ijtech.v15i1.6050

thickening fluid, which has a special microstructural change that leads to an improvement in energy absorption.

Shear thickening fluid (STF) is a type of non-Newtonian fluid consisting of oxide particles suspended in liquid polymers that respond to stress by increasing the viscosity, which is widely known as a hydro clustering mechanism (Haro, Szpunar, and Odeshi, 2016a). This mechanism explains that upon exposure to a high shear rate, nanoparticles cause repulsive loading by hydro clustering formation that packs together temporarily, forming a chain-like shape (Kim *et al.*, 2018). Furthermore, this mechanism explains that particles are pushed together by shear, and to move away from each other, and they must overcome the viscous drag forces from small lubrication gaps between neighboring particles (Brown and Jaeger, 2014). The principle implies that above a certain shear rate, the particles will grow into clusters, and the clustering mechanism results in a rise in viscosity which in turn acts like a solid (Hasanzadeh and Mottaghitalab, 2014). The previous study conducted by Agustha and Anne (2022) revealed that the impregnated Kevlar in STF mixed with TiC consistently demonstrated a higher impact value compared to composites with plain Kevlar due to the TiC nano-powder filling the space between the impregnated Kevlar fibers. Thus, the presence of TiC boosted the Kevlar's ability to absorb energy. Also, TiC nano-powder also strengthened the Kevlar's structure so its fibers would be unlikely to undergo shear stress, considering it would cost more energy to create fiber pull-out. Reinforcements with about 20 to 50 layers of woven aramid fibers are required to produce a high ballistic performance with respect to protection and energy absorption, in which STF can be incorporated into the composite system to reduce the number of layers of Kevlar fabric (Haro, Szpunar, and Odeshi, 2016b). Thus, the main objective of this research is to observe the energy absorption behavior of hybrid laminate composite impregnated with alumina, as a component of STF, with different thicknesses under both high velocity and low-velocity impact along with the type of deformation both on the aluminum surface and Kevlar fabric.

2. Methods

The method conducted in this research consists of sample fabrication and experimental testing.

2.1. Sample Fabrication

The process of fabricating hybrid laminate composites started with the preparation of materials. Aluminum alloy 7075-T6 sheet and Kevlar-29 were cut into the size of 7.5 x 15 cm for ballistic test samples and 55 x 10 mm dimensions for impact test samples. The chemical composition of aluminum alloy was 90.5% Al, 5.1-6 .1% % Zn, 2.1-2.9% Mg, 1.2-2% % Cu, and max. 0.5% Fe. The aluminum sheets' surfaces were cleaned by using sandpaper and ethanol to remove the impurities. The process was followed by the impregnation of Kevlar with shear thickening fluid (STF) consisting of alumina with 99.9% purity and 50 nm size supplied by Shanghai Xinglu Chemical Tech Co, LTD and PEG-400 with a 1:2 ratio following (Haro, Szpunar, and Odeshi, 2016a). The formulation is shown in Tables 1 and 2.

Table 1 Shear Thickening Fluid Formulation for Ballistic Test Sample

Kevlar Layers	Alumina (g)	PEG-400 (ml)	Ethanol (ml)
8	-	-	-
16	-	-	-
24	-	-	-
8	10	20	20
16	20	40	40
24	30	60	60

STF was produced by mixing an appropriate amount of alumina nanoparticles with polyethylene glycol (PEG-400) by using a magnetic stirrer for 1 hour at the speed of 1200 RPM. The process was continued by adding ethanol to the mixture and stirring again for another 1 hour. Kevlar fabrics that had been cut into desired dimensions were impregnated with STF. This step was followed by drying for 72 hours at room temperature to let the ethanol dry up (Haro, Szpunar, and Odeshi, 2016a). The composite assembly was done with the configuration shown in Figure 1. The hand lay-up method was used in the process of composite assembly. The adhesive used was a mixture of epoxy resin (Bisphenol A) and hardener with a ratio of 2:1. Pressure of 1600 Pa was given to the composite for 24 hours at room temperature (Haro, Szpunar, and Odeshi, 2016a).

Table 2 Shear Thickening Fluid Formulation for Impact Test Sample

Kevlar Layers	Alumina (g)	PEG-400 (ml)	Ethanol (ml)
8	-	-	-
16	-	-	-
24	-	-	-
8	1.47	2.94	2.94
16	2.94	5.88	5.88
24	4.41	8.82	8.82

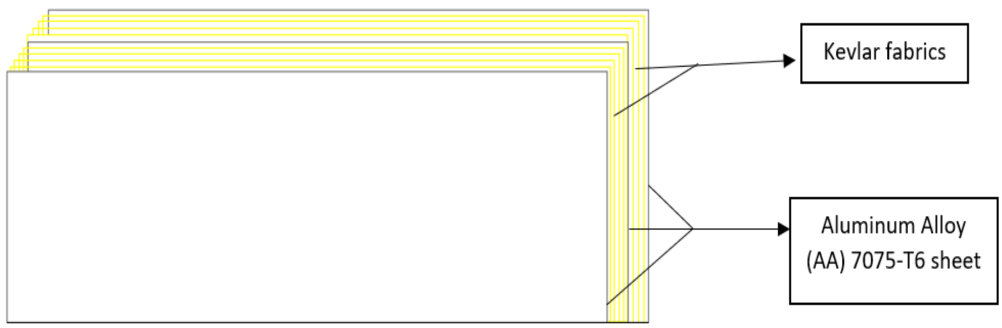

Figure 1 Configuration of AA7075/Kevlar-Al_2O_3 Hybrid Laminate Composite

2.2. Experimental Texting

2.2.1. Microstructural Analysis and Fourier Transform Infrared (FTIR) Spectrometry

Microstructural analysis was carried out on both impregnated and non-impregnated Kevlar samples to observe the dispersion of alumina nanoparticles using a scanning electron microscope (SEM). FTIR analysis was also performed on both samples to observe their respective functional groups. Both SEM imaging and FTIR analysis were conducted at the Center for Material Processing and Failure Analysis at Universitas Indonesia.

2.2.2. Ballistic Test

A ballistic impact test is categorized as a high-speed impact test that causes local response on targets due to insufficient time to distribute the energy. The test was performed by using a gun and projectile according to the NIJ 1080.01 standard level II, which are handgun (P1) and 9 x 19 mm projectile, named Parabellum, weighed 8 grams with a hemispherical tip. The initial velocity was 380 m/s with a 10 m distance. The energy absorbed by targets can be calculated by Equation 1 and 2 from the difference between the initial kinetic energy and the final kinetic energy as follows:

$$\text{Energy Absorbed (J)} = \frac{1}{2}\, m\, V_{initial}^{\;2} - \frac{1}{2}\, m\, V_{final}^{\;2} \quad (1)$$

$$\text{\%Absorbed Energy} = \left(\frac{residual\ energy}{initial\ energy}\right) x\ 100 \quad (2)$$

2.2.3. Impact Test

The impact test is categorized as low-velocity impact test leading to the global response. The test was performed by using the Charpy method according to ASTM E23. The maximum energy exerted by the pendulum was 300 J.

3. Results and Discussion

3.1. Analysis of Nanoparticles Presence and Dispersion

FTIR spectra of non-impregnated samples show several major absorption bands at wavelengths 3310.73, 1638.48, 1538.25, and 1303.33 cm^{-1}, presented in Figure 2. The wavelength of 3310.73 cm^{-1} corresponds to the presence of the N-H group, followed by the wavelength of 1638.48 $cm^{-1,}$ which indicates the presence of the amide carbonyl functional group (Ibrahim, Habib, and Jabrah, 2020). The wavelength of 1538.25 cm^{-1} is assigned as an N-H bond, while the peak at 1303.33 cm^{-1} represents the bonds of C-N and C-H bending (Ibrahim, Habib, and Jabrah, 2020).

As compared to non-impregnated Kevlar, the impregnated sample show peaks at 3393.36, 2876.31, 1643.14, 1092.12, and 511.31 cm^{-1}, shown in Figure 2. The peak at 3393.36 cm^{-1} is assigned as the terminal hydroxyl group of PEG since the impregnated Kevlar contains PEG as the constituent of STF (Gebregergs, 2018). The peaks at 2876.31, 1643.14, and 1092.17 cm^{-1} are responsible for the presence of C-H bands, C=O stretching, and C-O-C (Gebregergs, 2018; Chieng *et al.*, 2014; Polu and Kumar, 2011). The other prominent peak is at 511.31 $cm^{-1,}$ which is assigned to the Al-O bond, indicating the presence of alumina (Nila and Radha, 2018; Afruz and Tafreshi, 2014).

The dispersion of nanoparticles was observed under a scanning electron microscope, and the results are shown in Figure 3. Figures 3a and 3b demonstrate that individual Kevlar strands are arranged neatly, but some vacancies are present between them. These vacancies can lead to lower strength at a macroscopic scale. On the other hand, Figures 3c and 3d illustrate the presence of alumina nanoparticles that have agglomerated with a size of 350 nm, filling in the vacancies and covering some areas on the surface of Kevlar fibers due to their nanoscale size.

The effect of alumina nanoparticles' presence resulted in less amount of void, which increased the strength and energy absorption ability. This also facilitated stronger bonding of Kevlar fiber layers leading to stronger structure (Haro, Szpunar, and Odeshi, 2016a). The impregnation can strengthen fiber/matrix bonding and serve as a barrier to crack propagation, which in turn increases the penetration resistance (Haro, Szpunar, and Odeshi, 2016a).

It is apparent from Figure 3 that there are some agglomerated alumina nanoparticles surrounding Kevlar fibers. Nanoparticles have high surface area due to their smaller size, which leads to the increase in the Van der Waal attractive force on the particle surface, which attracts other particles to form a cluster that is referred to as the agglomeration process (Ilyas, Pendyala, and Marneni, 2016). The small size of nanoparticles brings both advantages and disadvantages, which is correlated to the high surface area. The disadvantage that can be seen in Figure 3 is the attractive interaction between the particles, resulting in agglomeration (Ashraf *et al.*, 2018). Another study explains that nanoparticles have an extremely high specific surface area, which makes them easy to agglomerate (Zhu and Ou, 2014).

3.2. Analysis of Kevlar Layer Amount and STF Impregnation to Ballistic Resistance

Figure 4a shows that the addition of Kevlar by 8 layers decreases the diameter of perforation by 5-7.3% within the category of non-impregnated and impregnated composite.

In addition, the presence of alumina nanoparticles due to the impregnation process decreased the diameter of perforation by 14.9-16.9% for the same amount of Kevlar layers compared to non-impregnated ones. It can be explained that the increase in thickness increased the energy absorption since more fibers need to be broken, which leads to higher accumulative energy absorption from each layer (Liu *et al.*, 2018).

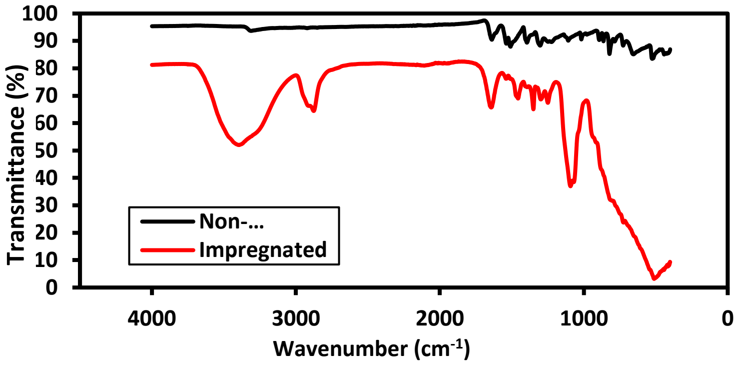

Figure 2 FTIR Spectra of Non-Impregnated and Impregnated Sample

Research shows that the increase in thickness leads to an increase in energy absorption ability (Talib *et al.*, 2012). The presence of STF that contained alumina nanoparticles also contributed to the perforation diameter. STF has such a mechanism that can resist the perforation when it is subjected to the projectile. Owing to the mechanism of hydro cluster formation, the viscosity of STF increases significantly in an instant. Hence, the high-viscosity fluid, in which the clusters enhance the hydrodynamic stress, is able to resist the energy to perforate the target (Haro, Szpunar, and Odeshi, 2016b).

The other parameter that can evaluate the ballistic performance is the depth of penetration, presented in Figure 4b. The measurement of penetration depth could only be done for impregnated samples as the non-impregnated samples were not penetrated well. The general trend for depth of penetration is increasing with the increase of Kevlar layers.

The low depth of penetration implies that the sample has less resistance to projectile penetration (Haro, Szpunar, and Odeshi, 2016a). In principle, as the number of layers increases, the composite is able to withstand energy exerted by projectiles. The energy received by the composite will be distributed within the composite. As a result, the energy absorption, which in this case is indicated by the depth of penetration, will be higher.

The depth of penetration is proportional to the energy absorbed, meaning that higher energy absorption can be observed by the high depth of penetration (Haro, Szpunar, and Odeshi, 2016a). However, the depth of penetration increases significantly for the 16-layers sample due to the presence of severely deformed parts. The deformed part was also included in the measurement as it occurred in the site where the depth of penetration could be measured. Meanwhile, the deformation in a 24-layers sample was not so severe. The difference in the severity of deformation can explain by the fact that although it had a lower depth of penetration than that of a 16-layers sample, the 24-layers sample had better resistance to a projectile, which will be further discussed in the next section. This shows that the energy absorption in a 24-layers sample was better as compared to a 16-layers sample.

3.3. Analysis of Deformation Behavior of Ballistic Targets

It can be compared that severe delamination took place in non-impregnated samples, while impregnated samples experienced less severe delamination, which mostly occurs at the front layers only. Delamination, which is shown in Figure 5a, b has such a characteristic where the constituent layers of composites are detached after being imposed to load. Delamination is assumed as an effect of interlaminar stress, and other theories state that delamination is a type of failure that occurs following the cracking of the matrix. The crack produces stress at the interface between the layers, which leads to delamination (Stefan *et al.*, 2020). Delamination has such a mechanism in which a fraction of compressive stress is reflected and becomes tensile stress, and the tensile wave causes crack initiation (Mohotti *et al.*, 2013).

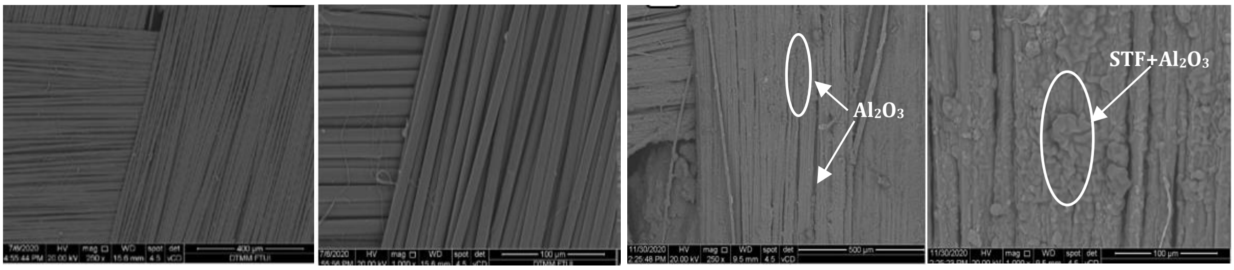

(a) (b) (c) (d)

Figure 3 SEM Observation Images of Non-Impregnated Kevlar (a,b) and impregnated Kevlar (c,d)

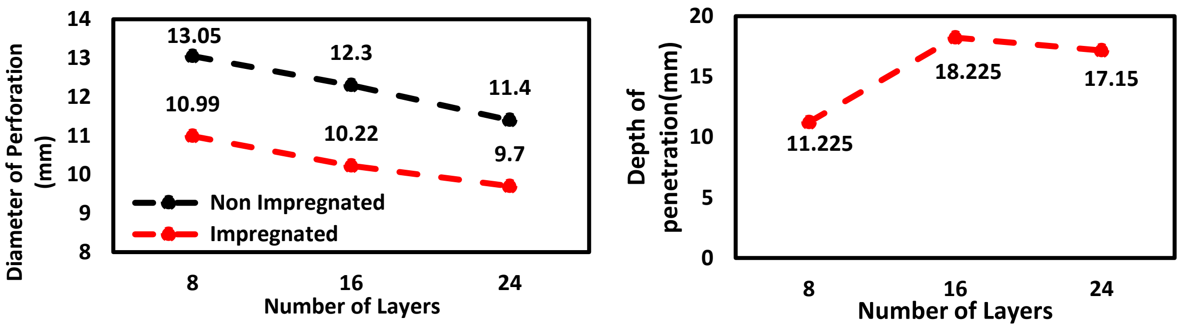

(a) (b)

Figure 4 Graphs of ballistic test: Diameter of Perforation (a); and Depth of Penetration (b)

However, impregnated samples with 24 layers of Kevlar did not experience delamination, as shown in Figure 5c. In impregnated samples, the clusters work to enhance hydrodynamic stress by increasing the viscosity in the suspension during impacts which contribute to the increase in delamination resistance as well as resistance to posterior crack propagation through load distribution between aluminum, resin, and the Kevlar fiber (Haro, Szpunar, and Odeshi, 2016b). In this case, the major delamination mode is a combination of adhesion and cohesion failure in which the adhesive layer remains on both surfaces of the Kevlar and aluminum sheet. As seen in Figure 5, the adhesion/cohesion delamination was dominated by adhesive failure. Furthermore, a study explains that delamination in impregnated samples is less intense since the targets have better adhesion with the aluminum sheet, resulting in more ductility and better resistance against projectile penetration.

Macroscopical photography was performed to better understand the phenomenon that cannot be seen from the outside part of the impregnated samples. Petalling can be seen in Figures 6a, b, and c, where the frontmost aluminum sheet created an open petal shape. This shape was formed due to the compressive load of the projectile that pushed the aluminum sheet to allow it to pass. The other type of deformation is plugging which can be seen in Figures 6b and c. It occurred in the second sheet of aluminum, which means that a fraction of the energy has been absorbed by the front layer. Normally, plugging results in the detachment of the metal part, but there is no evidence of such a failure in the sample. Instead, the sheet was pushed back by the projectile as a mechanism of energy absorption. Deformation due to compressive load from the projectile also took place at the back surface of the samples, known as bulging. Bulging occurs due to the remaining energy of the projectile that was absorbed by the backmost aluminum sheet. However, the energy was not sufficient to penetrate through it and only created a protruding spot in the sheet. Bulging can be seen clearly in Figure 6a. It is observed that bulging occurred in 8 and 16-layers composites. Figure 7 presents the back part of impregnated samples to better observe bulging.

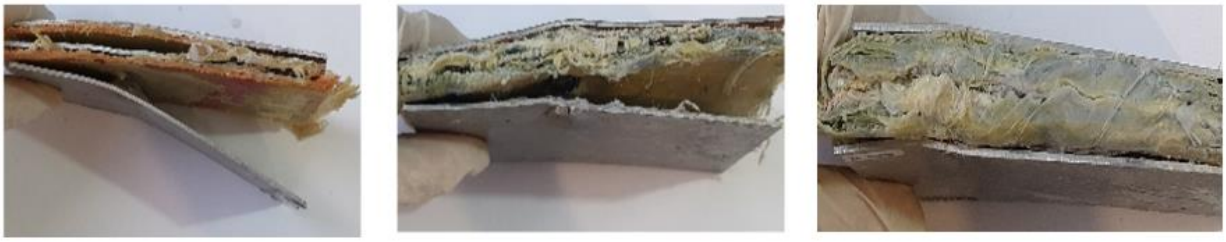

(a) (b) (c)

Figure 5 Delamination in 8-layers Non-Impregnated (a); Impregnated (b); 24-layers impregnated

Another thing that can be taken into consideration is the shape of the projectile nose. Research shows that a hemispherical nose shape tends to stretch the Kevlar fabric to failure instead of cutting through it by slipping through the fabric and pushing it against the other layer (Khodadadi *et al.*, 2019). The stretching of Kevlar in the ballistic sample is shown in Figure 8. Due to its high tensile strength, Kevlar is able to withstand the stretching effect from the projectile.

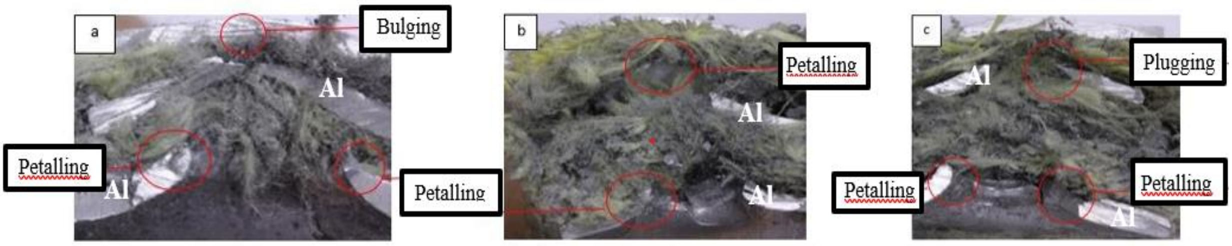

(a) (b) (c)

Figure 6 Macroscopic Photography of Impregnated Samples: 8-layers (a); 16 layers (b); 24 layers (c) after Ballistic Test

(a) (b) (c)

Figure 7 Kevlar Stretching upon perforation (a); Bulging in impregnated 8-layers (b); and 16-layers configurations

3.4. Analysis of Charpy Impact Test Result

The average impact energy data for composite impact samples are shown in Figure 8. Impact energy is the absorbed energy by each sample. The addition of a Kevlar layer leads to an increase in impact energy. Additionally, impregnated samples have a higher impact energy than that non-impregnated samples. Due to impregnation, there was an increase in impact energy by 18.2%, 17.4%, and 15.3% for 8-layers,16-layers, and 24-layers configurations, respectively. The highest energy absorption is seen in the 24-layers impregnated sample. The increase in energy absorption is caused by the presence of alumina nanoparticles, which contribute to the energy absorption mechanism.

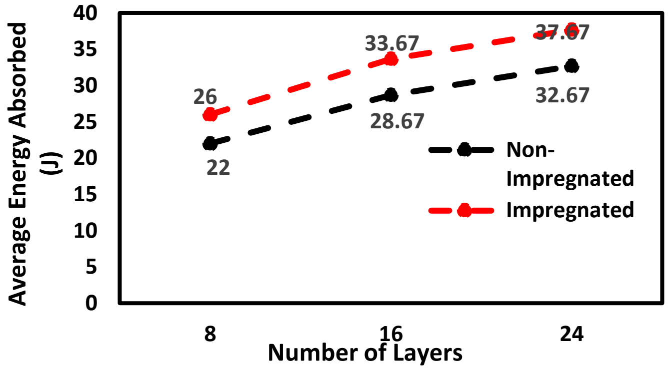

Figure 8 Graph of Average Impact Energy Absorption for Non-Impregnated and Impregnated Samples

All impact samples showed bending in the middle since the spots were hit by the pendulum, which can be seen in Figure 9. Non-impregnated sample with 8 layers of Kevlar experienced less deformation as it has a less delaminated part, and there is no sign of fracture or cracks on the aluminum sheet. On the other hand, the non-impregnated sample with 16 Kevlar layers delaminated more severely and experienced fracture in the frontmost aluminum sheet. Meanwhile, 24-layers non-impregnated samples show slight delamination, and there was no fracture.

The 8-layers and 16-layers configurations of impregnated samples show bending and delamination. Lastly, the 24-layers sample shows delamination, bending, and fracture. In impregnated samples, delamination may also occur due to the agglomeration of nanoparticles that block a part of the Kevlar area so that adhesive cannot completely reach Kevlar layers to hold it together with the aluminum alloy sheet. Since the size of the impact test sample is much smaller than that of ballistic samples, agglomeration has a serious adverse effect. Besides, delamination is majorly generated by interlaminar shear stresses, which are enhanced by the matrix cracks that induce stress at the ply interface (Stefan *et al.*, 2020). This condition is also supported by the global response due to low-velocity impact.

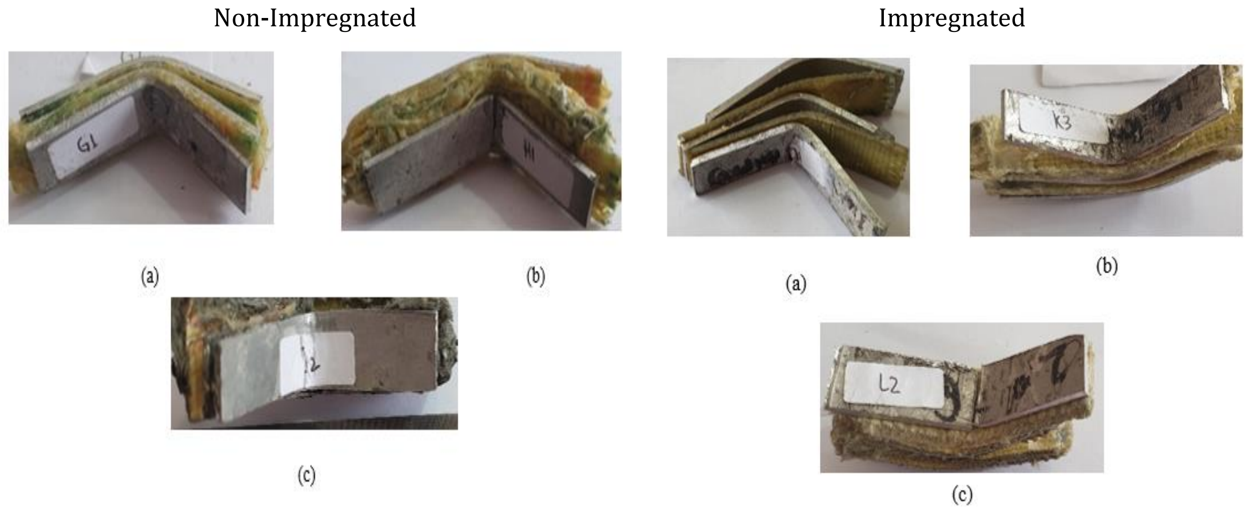

Figure 9 Macro photograph of Impact Test Results: 8 layers (a); 16 layers (b); and 24 layers (c)

4. Conclusions

The effects of STF impregnation on Kevlar were observed in hybrid laminate composites consisting of aluminum alloy 7075-T6, Kevlar, and epoxy resin with three variations of Kevlar layers amount. Microstructural analysis shows that alumina nanoparticles, as a constituent of STF, reduce the vacancies in between Kevlar fibers which translates to higher energy absorption ability. Some parameters that were investigated are perforation diameter, depth of penetration, and impact energy. The results show that impregnation with STF increases ballistic resistance and impact energy due to the hydro clustering mechanism, which facilitates the ability to resist perforation in ballistic test, which is categorized as high-velocity impact test. In addition, the presence of STF and its hydro clustering mechanism also generate higher energy absorption in impact test, which is categorized as low-velocity impact test. Besides, the increasing amount of Kevlar layers also contribute to ballistic resistance and energy absorption. The least severity of deformation mode from the ballistic test is observed on the 24-layers impregnated ballistic sample.

Acknowledgments

The authors would like to thank The Ministry of Research and Technology/National Research and Innovation Agency for financial support under PDUPT Grant with contract number: NKB-189/UN2.RST/HKP.05.00/2021.

References

Afruz, F.B., Tafreshi, M.J., 2014. Synthesis of γ-Al2O3 Nano Particles by Different Combustion Modes using Ammonium Carbonate. *Indian Journal of Pure and Applied Physics*, Volume 52(6), pp. 378–385

Agustha, F., Anne, Z.S., 2022, The Effect of Nano TiC Impregnation on Kevlars and The Number of Layers on Ballistic Properties of Laminate Hybrid Composite. *Suranaree Journal of Science & Technology,* Volume 29(2), p. 010123

Ashraf, M.A., Peng, W., Zare, Y., Rhee, K.Y., 2018. Effects of Size and Aggregation/Agglomeration of Nanoparticles on the Interfacial/Interphase Properties and Tensile Strength of Polymer Nanocomposites. *Nanoscale Research Letters,* Volume 13, pp. 1–7

Brown, E., Jaeger, H.M., 2014. Shear Thickening in Concentrated Suspensions: Phenomenology, Mechanisms and Relations to Jamming. *Reports on Progress in Physics,* Volume 77(4), p. 046602

Chieng, B.W., Ibrahim, N.A., Yunus, W.M.Z.W., Hussein, M.Z., 2014. Poly(lactic acid)/Poly(ethylene glycol) Polymer Nanocomposites: Effects of Graphene Nanoplatelets. *Polymers,* Volume 6(1), pp. 93–104

Gebregergs, A., 2018. *Synthesis and Characterization of Cellulose-Based Hydrogels Using Citric Acid as a Crosslinker*. Addis Ababa University Addis, Ethiopia

Haro, E.E., Szpunar, J.A., Odeshi, A.G., 2016a. The Energy Absorption Behavior of Hybrid Composite Laminates Containing Nano-Fillers Under Ballistic Impact. *International Journal of Impact Engineering,* Volume 96, pp. 11–22

Haro, E.E., Szpunar, J.A., Odeshi, A.G., 2016b. Ballistic Impact Response of Laminated Hybrid Materials Made of 5086-H32 Aluminium Alloy, Epoxy and Kevlar® Fabrics Impregnated with Shear Thickening Fluid. *Composites Part A: Applied Science and Manufacturing,* Volume 87, pp. 54–65

Hasanzadeh, M., Mottaghitalab, V., 2014. The Role of Shear-Thickening Fluids (STFs) in Ballistic and Stab-Resistance Improvement of Flexible Armor. *Journal of Materials Engineering and Performance,* Volume 23(4), pp. 1182–1196

Ibrahim, M.B., Habib, H.Y., Jabrah, R.M., 2020. Preparation of Kevlar-49 Fabric/E-Glass Fabric/Epoxy Composite Materials and Characterization of Their Mechanical Properties. *Revue Des Composites et Des Materiaux Avances*, Volume 30(3–4), pp. 133–141

Ilyas, S.U., Pendyala, R., Marneni, N., 2016. Stability and Agglomeration of Alumina Nanoparticles in Ethanol-Water Mixtures. *Procedia Engineering,* Volume 148, pp. 290–297

Khodadadi, A., Liaghat, G., Bahramian, A.R., Ahmadi, H., Anani, Y., Asemani, S., Razmkhah, O., 2019. High Velocity Impact Behavior of Kevlar/Rubber and Kevlar/Epoxy Composites: A Comparative Study. *Composite Structures,* Volume 216, pp. 159–167

Kim, Y.H., Park, Y., Cha, J.H., Ankem, V.A., Kim, C.G., 2018. Behavior of Shear Thickening Fluid (STF) Impregnated Fabric Composite Rear Wall Under Hypervelocity Impact. *Composite Structures,* Volume 204, pp. 52–62

Liu, L., Zhao, Z., Chen, W., Luo, G., 2018. Influence of Pre-Tension on Ballistic Impact Performance of Multi-Layer Kevlar 49 Woven Fabrics for Gas Turbine Engine Containment Systems. *Chinese Journal of Aeronautics,* Volume 31(6), pp. 1273–1286

Mohotti, D., Ngo, T., Mendis, P., Raman, S.N., 2013. Polyurea Coated Composite Aluminium Plates Subjected to High Velocity Projectile Impact. *Materials & Design,* Volume 52, pp. 1–16

Nila, A.S.S., Radha, K., 2018. Synthesis and XRD, FTIR Studies of Alumina Nanoparticle using Co-precipitation Method. *International Journal for Research in Applied Science and Engineering Technology,* Volume 6(3), pp. 2493–2496

Polu, A.R., Kumar, R., 2011. Impedance Spectroscopy and FTIR Studies of PEG - Based Polymer Electrolytes. *E-Journal of Chemistry,* Volume 8(1), pp. 347–353

Senthil, K., Iqbal, M.A., Chandel, P.S., Gupta, N.K., 2017. Study of The Constitutive Behavior Of 7075-T651 Aluminum Alloy. *International Journal of Impact Engineering,* Volume 108, pp. 171–190

Stefan, A., Pelin, G., Dragomirescu, A., Petre, A., Ilina, S., 2020. Delamination Mechanisms in Fiber-Reinforced Composites Structures Tested at Different Loadings. *INCAS Bulletin,* Volume 12(1), pp. 175–182

Talib, A.R.A., Abbud, L.H., Ali, A., Mustapha, F., 2012. Ballistic Impact Performance of Kevlar-29 and Al2O3 Powder/Epoxy Targets under High Velocity Impact. *Materials and Design,* Volume 35, pp. 12–19

Yeter, E., 2018. Investigation of Ballistic Impact Response of Aluminum Alloys Hybridized with Kevlar/Epoxy Composites. *Politeknik Dergisi,* Volume 22(1), pp. 219–227

Zhu, Q. W., Ou, M.G., 2014. The Function of PEG in The Synthesis of Nanomaterials. *Applied Mechanics and Materials,* Volume 670, pp. 3–9